Eur. Phys. J. Special Topics **226**, 705–723 (2017)

DOI: 10.1140/epjst/e2016-60326-1

THE EUROPEAN PHYSICAL JOURNAL SPECIAL TOPICS

Regular Article

Comparison of Boltzmann and Gibbs entropies for the analysis of single-chain phase transitions

T. Shakirov[1], S. Zablotskiy[2], A. Böker[1], V. Ivanov[2], and W. Paul[1,a]

[1] Institut für Physik, Martin-Luther-Universität Halle-Wittenberg, 06099 Halle (Saale), Germany
[2] Faculty of Physics, Moscow State University, Moscow 119991, Russia

Received 14 October 2016 / Received in final form 12 December 2016
Published online 5 April 2017

Abstract. In the last 10 years, flat histogram Monte Carlo simulations have contributed strongly to our understanding of the phase behavior of simple generic models of polymers. These simulations result in an estimate for the density of states of a model system. To connect this result with thermodynamics, one has to relate the density of states to the microcanonical entropy. In a series of publications, Dunkel, Hilbert and Hänggi argued that it would lead to a more consistent thermodynamic description of small systems, when one uses the Gibbs definition of entropy instead of the Boltzmann one. The latter is the logarithm of the density of states at a certain energy, the former is the logarithm of the integral of the density of states over all energies smaller than or equal to this energy. We will compare the predictions using these two definitions for two polymer models, a coarse-grained model of a flexible-semiflexible multiblock copolymer and a coarse-grained model of the protein poly-alanine. Additionally, it is important to note that while Monte Carlo techniques are normally concerned with the configurational energy only, the microcanonical ensemble is defined for the complete energy. We will show how taking the kinetic energy into account alters the predictions from the analysis. Finally, the microcanonical ensemble is supposed to represent a closed mechanical N-particle system. But due to Galilei invariance such a system has two additional conservation laws, in general: momentum and angular momentum. We will also show, how taking these conservation laws into account alters the results.

Flat histogram Monte Carlo (MC) simulations like multi-canonical simulations [1–4], Wang-Landau simulations [5–7] or Stochastic Approximation Monte Carlo (SAMC) simulations [8–10] allow for the determination of the density of states $g(U)$ of a model, where U is the configurational (potential) energy, as MC simulations normally live in configuration space not in phase space. Typically, these simulations are limited

[a] e-mail: Wolfgang.Paul@physik.uni-halle.de

to rather small system sizes N. The analysis of the pseudo-phase behavior of these small finite systems relies on the evaluation of singular points in the thermodynamic functions obtainable from the density of states. For this analysis, a combined approach in the canonical and the microcanonical ensemble [11] has proven most powerful, also for polymeric systems [12–14] (a recent review can be found in [15]).

To link a statistical observable like the density of states (i.e., the number of states at fixed configurational energy, $g(U)$, or at fixed total energy, $g(E)$) to thermodynamics is the task of statistical physics. The linking physical observable is the entropy, S, a quantity of central importance in statistics as well as in thermodynamics. In thermodynamics it is one of the so-called macroscopic observables of a system, and one distinguishes between the micro-state of the system (its configuration or the point in phase space representing the system) and the macro-state of the system. For a simple thermodynamic system, the latter is given by fixing three variables, e.g., the number of particles, N, the volume of the system, V, and the energy of the system, E. The thus specified ensemble is called the microcanonical ensemble of statistical physics. Thermodynamics establishes relations between the differentials of these macroscopic variables, e.g., the Gibbs fundamental form

$$dE = TdS - pdV + \mu dN. \tag{1}$$

The prefactors are given by the intensive thermodynamic variables temperature, T, pressure, p, and chemical potential, μ. All functions occurring in this equation are macro-variables and, for this equation (and equivalent formulations) to make sense, have to be differentiable functions. Obviously, this can not be true for the particle number, and clearly it is also not true when we consider the energy to be given for a quantum system with discrete energy levels. One therefore typically considers this equation to hold for large systems in a suitable thermodynamic limit, where the discreteness of some of the variables can be (hopefully) neglected. For finite systems, equation (1) should be read as an empirical relation between finite differences

$$\Delta E = T\Delta S - p\Delta V + \mu\Delta N, \tag{2}$$

established experimentally by the founders of thermodynamics. Mathematically, the existence of differential thermodynamic relations like equation (1) is based on large deviation theory [16,17]. When the probability for the occurrence of a macro-variable, X, behaves as $\rho(X) \simeq \exp\{-Nr(X)\}$ with some rate function, $r(X)$, then for $N \to \infty$ only the state with the minium $r(X)$ (i.e., maximum $\rho(X)$) will contribute. If we take $X = E$ then $r(X) = -s(E)$ is the negative entropy per particle, i.e., only the state with the maximum entropy is relevant in the thermodynamic limit. Such an argument was also used in the work by Hertz [18,19], who presented a derivation of thermodynamics from statistical mechanics based on Gibbs [20] earlier work. Clearly, the mathematical background for the derivation of thermodynamic laws via large fluctuation theory does not rely on the existence of an underlying mechanical picture, be it classical or quantum. This explains the general applicability of thermodynamics. Nevertheless, a closed mechanical N-particle system is the archetypical system for which thermodynamic relations are considered to hold, and notwithstanding the questions about the discreteness of some thermodynamic variables, it is important to understand for such a system, how the link between statistics and thermodynamics should be constructed, i.e., how entropy should be defined statistically.

Regarding this question, some recent works by Hilbert, Dunkel and Hänggi [21–25] have raised a controversy in the literature [26,27]. Hilbert, Dunkel and Hänggi pointed out that entropy is an adiabatic invariant in thermodynamics and consequently should be defined statistically for a mechanical N-particle system by a quantity which is a mechanical adiabatic invariant [28], which all are related to the existence of action-angle

variables in mechanics [29]. Concerning the density of states, which is the quantity we are aiming at with our simulations, it has been noted early on [18,19,30] that the density of states itself, i.e., the integral over the hyperplane in phase space for fixed energy, is not an adiabatic invariant

$$W(E) = \int_{H(x)=E} d\sigma(x). \tag{3}$$

Here $x = (\mathbf{q}_1, \ldots, \mathbf{q}_N, \mathbf{p}_1, \ldots, \mathbf{p}_N) \in \Gamma$ is a point in phase space Γ, and the integral is performed using the surface element, $d\sigma(x)$, on the surface of constant energy, $H(x) = E$. Relating the entropy to the logarithm of this density of states (typically assigned to Boltzmann and therefore called Boltzmann entropy, we set $k_B = 1$)

$$S_B(E) = \ln W(E) \tag{4}$$

therefore also does not lead to an adiabatically invariant entropy [24,25,31]. Note, however, that the correct probability density on a surface of constant energy is proportional to $d\sigma(x)/|\nabla H(x)|$ [18,19,30] with the normalization given by the density of states

$$g(E) = \int_{H(x)=E} d\sigma(x)/|\nabla H(x)| \,. \tag{5}$$

This is, however, still not an adiabatically invariant quantity [30]. For a system with discrete energy spectrum and/or discrete state space like an Ising model, the Boltzmann definition equation (3) and the definition in equation (5) become equivalent. Both definitions are furthermore local in energy (i.e., defined for a hypersurface of constant energy) and we will therefore in the following also use

$$S_B(E) = \ln g(E) \tag{6}$$

to denote the Boltzmann entropy in our calculation (see also the discussion in the model section). Using the divergence theorem, it is easy to see that one can write

$$\Omega(E) = \int^E g(E')dE' = \int^E dE' \int_{H(x)=E'} \frac{d\sigma(x)}{|\nabla H(x)|} = \int_{H(x)\leq E} dx \tag{7}$$

i.e., $\Omega(E)$ is the integral over all points in phase space with energy smaller than E. The Gibbs definition of entropy

$$S_G(E) = \ln \Omega(E) \tag{8}$$

leads to an adiabatic invariant [18–20,30]. For systems fulfilling the conditions of the Gärtner-Ellis theorem [16], in the thermodynamic limit all three entropy definitions yield the same thermodynamic relations. For finite systems, however, their predictions somewhat differ, the most notable difference being that for models with a finite upper energy bound, the Boltzmann entropy leads to a region of negative values for the microcanonical temperature, $T_B^{-1}(E) = dS_B(E)/dE$, whereas the temperature derived from the Gibbs entropy, $T_G^{-1}(E) = dS_G(E)/dE$, is always positive. Hilbert, Dunkel and Hänggi also showed [24,25] that for small mechanical systems thermal equilibrium between two systems is related to the equality of the Gibbs temperature $T_G(E)$, not the Boltzmann temperature, $T_B(E)$. Keep in mind however, that all these derivations are based on an application of the thermodynamic relations between differentials, equation (1); Hilbert, Dunkel and Hänggi are well aware of the problems which can arise for discrete energy values, but do not discuss the discreteness of

the particle number in the microcanonical ensemble. Here we will not enter into any further argument about what is the correct definition of entropy, as this is not the thrust of this paper, but will focus on the consequences of choosing the two different definitions for two non-trivial finite polymeric model systems.

Another point, which we would like to elucidate, concerns the effect of some negligence regarding the effect of Galilei invariance on the definitions in equation (3) and equation (5). Due to Galilei invariance, a closed mechanical N-particle system has (at least) two more conservation laws besides the energy conservation: total momentum and total linear momentum are also conserved (for an integrable system, there exists of course a complete set of conserved quantities – the angle variables – all related to adiabatic invariants of the motion [29]). The motion of the N-particle system therefore does not cover the complete surface of constant energy as assumed above. Assuming hard, infinitely heavy container walls (NVE ensemble) linear momentum and angular momentum are no longer conserved, whereas for a NVE simulation using periodic boundary conditions one would retain the conservation of linear momentum. Following Schierz et al. [32] one can ask what consequences the presence of these conservation laws would have on the analysis of flat-histogram simulations. And finally, considering flat histogram Monte Carlo simulations, one generally considers the density of states in configuration space, $g(U)$, not of the total energy $g(E)$ with $E = U + K$, K being the kinetic energy. What is the effect of neglecting the kinetic energy on the predictions concerning, e.g., the phase behavior of the model?

Our paper is organized as follows. In Section 1 we provide the theoretical background for the calculation of the density of states $g(E)$ from the configurational density of states $g(U)$ determined in the simulations in the presence of the different conservation laws. Section 2 will describe the two polymer models which we have used to exemplify the predictions obtained from using either the Boltzmann or the Gibbs entropy for small systems. In Section 3 we will present our results for our two polymer model systems. Finally, Section 4 presents our conclusions.

1 Theoretical background

As discussed in the introduction, Monte Carlo simulations are performed in configuration space and, consequently, the density of states one obtains is the configurational one, $g(U)$. One can perform a combined canonical-microcanonical analysis based on this density of states, and contrasting the Gibbs entropy, $S_G(U) = \ln \Omega(U)$, and the Boltzmann entropy, $S_B(U) = \ln g(U)$, where $\Omega(U) = \int_{U_{min}}^{U} g(U')dU'$, where U_{min} is the lowest energy to which the density of states converged in the simulation. Typically, one does not reach the ground state with a converged $g(U)$, but stays a few percent above, however, covering the range of energies contributing to thermal pseudo phase transitions in the model. The configurational microcanonical temperatures in the two cases are given by $T_B^{-1}(U) = dS_B(U)/dU$ and $T_G^{-1}(U) = dS_G(U)/dU$. The predictions for the Gibbs and Boltzmann entropies in configuration space are contrasted in Section 3.1.

1.1 Density of states in phase space

The definition of the thermodynamic quantities according to Boltzmann or Gibbs remains identical to the discussion above, one only has to exchange the configurational energy for the total energy $E = U + K$. The question which has to be addressed therefore is how to calculate the density of states, $g(E)$, in phase space

from the density of states, $g(U)$, in configuration space that is determined numerically in the simulations [33]. For given K and U the number of possible states is $g_2(U,K) = g_{id}(K) \cdot g(U)$, where g_{id} is the number of possible momentum combinations giving kinetic energy K. The density of states $g(E)$ can then be found by integration

$$g(E) = \int_{U_{\min}}^{U_{\max}} \mathrm{d}U \int_0^\infty \mathrm{d}K \; g_2(U,K)\, \delta(E-K-U)$$

or in the case of a discrete spectrum of potential energies, on which we will focus in the following as this is the case for the two models we are discussing here

$$g(E) = \sum_{U=U_{\min}}^{U_{\max}} \int_0^\infty \mathrm{d}K \; g_2(U,K)\, \delta(E-K-U). \tag{9}$$

Here $U_{\min}$ and $U_{\max}$ are the minimal and maximal configurational energies possible (resp. considered). This can be written as

$$\begin{aligned} g(E) &= \sum_{U=U_{\min}}^{U_{\max}} \int_0^\infty \mathrm{d}K \; g(U)\, g_{id}(K)\, \delta(E-K-U) \\ &= \sum_{U=U_{\min}}^{U_{\max}} g(U)\, g_{id}(E-U)\, \Theta(E-U), \end{aligned} \tag{10}$$

where Θ is the Heaviside step-function.

Since g_{id} depends only on the linear momenta ($2mK = \sum_i \boldsymbol{p}_i^2$), for N particles it is proportional to the area of a hypersphere in d-dimensional space

$$g_{id}(K) \propto K^{d/2-1}. \tag{11}$$

The exact value of the proportionality factor is not important for us, because the configurational density of states is estimated by SAMC simulations, which only yield information up to an unknown prefactor also. The value of the exponent depends on what other conservation laws besides energy conservation are considered. It is $d = 3N$ for N particles in 3-dimensional space and $d = (3N-3)$ for N particles in 3-dimensional space with the total linear momentum conservation. The case of angular momentum conservation is more involved and will be considered in more detail below.

Combining equation (10) and equation (11) we obtain

$$\begin{aligned} g(E) &\propto \sum_{U=U_{\min}}^{U_{\max}} (E-U)^{d/2-1}\, g(U)\Theta(E-U) \\ &= \sum_{U=U_{\min}}^{U_{\max}} \exp\left\{\left(\frac{d}{2}-1\right)\ln(E-U) + \ln g(U)\right\}\Theta(E-U). \end{aligned} \tag{12}$$

These expressions can be evaluated numerically for any $E \geq U_{\min}$.

To calculate the Gibbs entropy, we should consider the total number of states with energy less than E.

$$\Omega(E) = \int_{U_{\min}}^{E} dE' g(E') = \int_{U_{\min}}^{E} dE' \sum_{U=U_{\min}}^{U_{\max}} g(U)\, g_{id}(E'-U)\, \Theta(E'-U). \tag{13}$$

By taking into account (11)

$$\Omega(E) \propto \int_{U_{\min}}^{E} dE' \sum_{U=U_{\min}}^{U_{\max}} g(U)\,(E'-U)^{d/2-1}\,\Theta(E'-U)$$
$$= \sum_{U=U_{\min}}^{U_{\max}} g(U) \int_{U}^{E} dE'\,(E'-U)^{d/2-1}\,\Theta(E'-U) \tag{14}$$

or after integration

$$\Omega(E) \propto \sum_{U=U_{\min}}^{U_{\max}} g(U)\,(E-U)^{d/2}\,\Theta(E-U) \tag{15}$$

which is similar to equation (12) except for the exponent of $(E-U)$ which is larger by 1 for the Gibbs entropy. It means that all relations derived below for derivatives of the Boltzmann entropy can be applied to the Gibbs entropy after replacing $(d/2-1)$ by $d/2$. For the inverse microcanonical temperature we obtain from equation (12)

$$T_B^{-1}(E) = \frac{d\ln g}{dE} = \frac{g'(E)}{g(E)}$$
$$= \frac{1}{g(E)} \sum_{U=U_{\min}}^{U_{\max}} g(U) \left[\left(\frac{d}{2}-1\right)(E-U)^{d/2-2}\,\Theta(E-U) \right. \tag{16}$$
$$\left. + (E-U)^{d/2-1}\delta(E-U) \right].$$

The second term in the sum of equation (16) is non-analytic, but has no contribution to $T_B^{-1}(E)$ for positive exponent $d/2-1$:

$$T_B^{-1}(E) = \frac{1}{g(E)} \left(\frac{d}{2}-1\right) \sum_{U=U_{\min}}^{U_{\max}} g(U)\,(E-U)^{d/2-2}\,\Theta(E-U)\,. \tag{17}$$

The summation in equation (17) can be done numerically similarly to the summation in equation (12). In the microcanonical analysis we also need the determination of maxima and minima and inflection points of the inverse temperature. The first derivative of $T_B^{-1}(E)$ is given by

$$\frac{dT_B^{-1}(E)}{dE} = \frac{d^2\ln g(E)}{dE^2} = \frac{g''(E)}{g(E)} - \left(\frac{g'(E)}{g(E)}\right)^2 = \frac{g''(E)}{g(E)} - \left(T_B^{-1}(E)\right)^2 \tag{18}$$

where after neglecting the non-analytical terms we obtain

$$g''(E) = \left(\frac{d}{2}-1\right)\left(\frac{d}{2}-2\right) \sum_{U=U_{\min}}^{U_{\max}} g(U)\,(E-U)^{d/2-3}\,\Theta(E-U). \tag{19}$$

Finally, the 2nd derivative of $T_B^{-1}(E)$ is given by

$$\frac{d^2T_B^{-1}(E)}{dE^2} = \frac{d^3\ln g(E)}{dE^3} = \frac{g'''(E)}{g(E)} - 3\frac{dT_B^{-1}(E)}{dE}T_B^{-1}(E) - \left(T_B^{-1}(E)\right)^3 \tag{20}$$

where similarly

$$g'''(E) = \left(\frac{d}{2}-1\right)\left(\frac{d}{2}-2\right)\left(\frac{d}{2}-3\right)\sum_{U=U_{\min}}^{U_{\max}} g(U)\,(E-U)^{d/2-4}\,\Theta(E-U)\,. \quad (21)$$

As stated above, the results for the inverse microcanonical temperature $T_G^{-1}(E)$ according to Gibbs can be obtained from above equations for the Boltzmann temperature by replacing $d/2-1$ by $d/2$.

1.2 Conservation of angular momentum

To take into account the conservation of angular momentum one needs to go back to the definition of the density of states as an integral over phase space,

$$g(E) \propto \int dq^{3N}\,(E-U(q))^{d/2-1}\,\Theta(E-U(q))\,, \quad (22)$$

where we have already performed the integration over the momenta. The value of the number of degrees of freedom, d, depends on the conservation laws considered. Equation (22) corresponds to a system with total energy conservation only. In the presence of additional conservation laws, equation (22) should be modified, because of the reduction of the degrees of freedom and the change in integration variables. When changing the variables, one needs in general to multiply the integrand by a Jacobi determinant. In the case of linear momentum conservation, the determinant does not depend on the coordinates of the particles, i.e. it is just a numerical factor, and it can be included for the calculation of $g(E)$ in the proportionality factor which we ignore. But in the case of angular momentum conservation, the determinant depends on the coordinates and can not be ignored. For the case of both linear and angular momentum conservation, equation (22) should be modified as (see for instance [32])

$$g(E) \propto \int \frac{dq^{3N}}{\sqrt{\det I(q)}}\left(E-U(q)-\frac{\mathbf{P}^2}{2M}-\frac{1}{2}\mathbf{J}^T I^{-1}(q)\mathbf{J}\right)^{d/2-1} \Theta\left(E-U(q)-\frac{\mathbf{P}^2}{2M}-\frac{1}{2}\mathbf{J}^T I^{-1}(q)\mathbf{J}\right), \quad (23)$$

where $d=3N-6$, M is the total mass of the system, $I(q)$ is the inertia tensor depending on the particle coordinates q, $\mathbf{J}$ is the the total angular momentum, and $\mathbf{P}$ is the the total linear momentum. The latter two are constants. In the simplest case we choose $\mathbf{P}=0$ (can be done due to Galilei invariance) and also $\mathbf{J}=0$ and get

$$g(E) \propto \int \frac{dq^{3N}}{\sqrt{\det I(q)}}\,(E-U(q))^{d/2-1}\,\Theta(E-U(q))\,. \quad (24)$$

In the case of a discrete spectrum of the configurational energy, equation (24) can be written as

$$g(E) \propto \sum_{U=U_{\min}}^{U_{\max}} \int \frac{dq^{3N}}{\sqrt{\det I(q)}}\,(E-U)^{d/2-1}\,\Theta(E-U)\,\delta(U(q)-U)\,. \quad (25)$$

Only the δ-function and the determinant depend on the configuration, and equation (25) can be rewritten as

$$g(E) \propto \sum_{U=U_{\min}}^{U_{\max}} (E-U)^{d/2-1}\,\Theta(E-U)\int \frac{dq^{3N}}{\sqrt{\det I(q)}}\,\delta(U(q)-U)\,. \quad (26)$$

The integral is proportional to the average value of $1/\sqrt{\det I}$. The number of microstates corresponding to the configurational energy U is $g(U)$, and the probability of a microstate is $1/g(U)$. Then $p(q|U) = \delta(U(q) - U)/g(U)$ is the conditional probability density to find the system in point q in configuration space where it has the configurational energy U

$$\int \frac{dq^{3N}}{\sqrt{\det I(q)}} \delta(U(q) - U) = g(U) \int \frac{dq^{3N}}{\sqrt{\det I(q)}} \frac{\delta(U(q) - U)}{g(U)}$$
$$= g(U) \int \frac{dq^{3N}}{\sqrt{\det I(q)}} p(q|U) = g(U) \left\langle \frac{1}{\sqrt{\det I}} \right\rangle_U, \tag{27}$$

where $\langle \cdots \rangle_U$ denotes the averaging at given configurational energy U. The value of $\left\langle 1/\sqrt{\det I} \right\rangle_U$ in equation (27) can be estimated in a standard way in a SAMC productive run [15].

2 Models and simulation techniques

We describe in this section two models which we have used to exemplify the thermodynamic predictions for small systems using either the Gibbs or the Boltzmann entropy.

2.1 Model of a single semiflexible-flexible (SF) copolymer chain

We are considering single multi-block-copolymer chains consisting of an equal amount of flexible (F) and semi-flexible (S) blocks of beads of diameter σ. The chain length is fixed at $N = 64$, the block length can be varied. The bond length is allowed to change freely in the small interval $[0.8\sigma, 1.25\sigma]$, enabling elementary shift moves of monomers and keeping the excluded volume condition fulfilled. In such a model the momenta of the beads are not constraint. Stiffness is introduced into the model by a square-well potential favoring bond angles in the interval $[150°, 170°]$. Non-valent interactions are also of square well type and are equal between all monomer types, the square well width being $\lambda = 1.5$ in units of the monomer diameter $\sigma = 1$. Calling n_{st} the number of angles in the preferred interval and n_{nv} the number of monomer pairs with a distance smaller than λ, the energy of a configuration is given by

$$U = -\varepsilon n_{nv} - \varepsilon_{st} n_{st}, \tag{28}$$

where ε_{st} is the energy scale for the bending energy. We set $\varepsilon = 1$ as the energy scale of the model and can then consider phase behavior in the plane $\varepsilon_{st}/\varepsilon, \varepsilon/T$. Results on the state diagram of this model have been reported in references [34–36]. Technically, we determined a two-dimensional density of states $g(n_{nv}, n_{st})$ from which the configurational density of states is then calculated as $g(U) = \sum'_{n_{nv}, n_{st}} g(n_{nv}, n_{st})$. Here the sum is over all pairs (n_{nv}, n_{st}) fullfilling the condition $U = -\varepsilon n_{nv} - \varepsilon_{st} n_{st}$.

2.2 Model of poly-alanine (PRIME20)

The PRIME20 model was first published in reference [37] in 2010 as an extension to PRIME (Protein Intermediate-Resolution Model) [38], developed by the same group

in 2001. While PRIME was mostly used to model poly-alanines, PRIME20 is designed to include all 20 proteinogenic amino acids.

Each amino acid is represented by four beads or "united atoms", one each for the backbone amino group (N), the alpha carbon (C_α), the carboxyl group (C), and the side chain (R). Bonds between these beads fluctuate freely within a narrow range around their ideal length. Bond angles, L-isomerization of amino acids and *trans* configuration of the peptide bond are imposed by pseudo-bonds with the same characteristics between next neighbors as well as between two neighboring C_α beads.

All non-bonded beads interact by a hard-sphere repulsion. Side chain beads have an additional square-well interaction whose strength depends on the interacting types. To limit parameter space, the 20 different side chains are classified into 14 groups depending on their properties such as polarity, charge, or the capability to form hydrogen bonds. This way, the model only requires 19 energy parameters (i.e. well depths) compared to up to 171 if each pair of side chains (discounting Glycine) were assigned one parameter. Backbone (N-C) hydrogen bonds are modeled as a square well with additional restraints: the involved N-H-O and C-O-H angles (H and O positions are determined on demand) must be sufficiently straight, neither partner may be part of another hydrogen bond, and they must be separated by at least 3 intervening amino acids. If all these criteria are met, a hydrogen bond is formed with a well depth $\epsilon_{HB} = -1$, which dominates the energy function as all side chain energy parameters are between -0.585 (Cys-Cys interaction) and $+0.253$ (repulsion of charged side chains). In this paper we focus on poly-alanines, which means that the side chain well depth is always $\epsilon_{AA} = -0.084$, and determine the configurational density of states $g(U)$ from the simulation.

2.3 SAMC algorithm

The Stochastic approximation Monte Carlo (SAMC) algorithm [8–10] is a recently suggested mathematical generalization of the Wang-Landau (WL) algorithm [5–7] with proven convergence to the true density of states. It is an iterative procedure, optimizing an estimate for the density of states of a model system. Its applicability for polymer systems has been established in references [34–36,39,40]. A Monte Carlo simulation using a converged estimate for the density of states from this procedure leads to a random walk over the allowed energies of the model system. During such a simulation, averages of observables at fixed energy $\overline{A}(E)$ can be obtained. Their temperature dependence in the canonical ensemble can then be calculated as

$$\langle A \rangle(T) = \frac{1}{Z(T)} \int g(E)\overline{A}(E) \exp\{-\beta E\} dE, \tag{29}$$

where $\beta = 1/k_B T$ and $Z(T)$ is the canonical partition function.

Finally, let us stress that it is important to be aware of the influence of the numerical implementation of the density of states determination on the interpretation of the results. For the SF copolymer, we can determine a density of states as a function of a discrete configurational energy, $g(U_i)$, for the poly-alanine with its many different energy parameters, we select a discretization of the relevant configurational energy range $[U_{\min}, U_{\max}]$ in intervals of width ΔU. In the former case we determine the number of states at fixed energy, i.e., the realization of equation (3). In the latter case, we are determining the number of states in configuration space belonging to energies in the interval $[U, U + \Delta U]$, which is a volume $\Delta\mathcal{V}$ in configuration space.

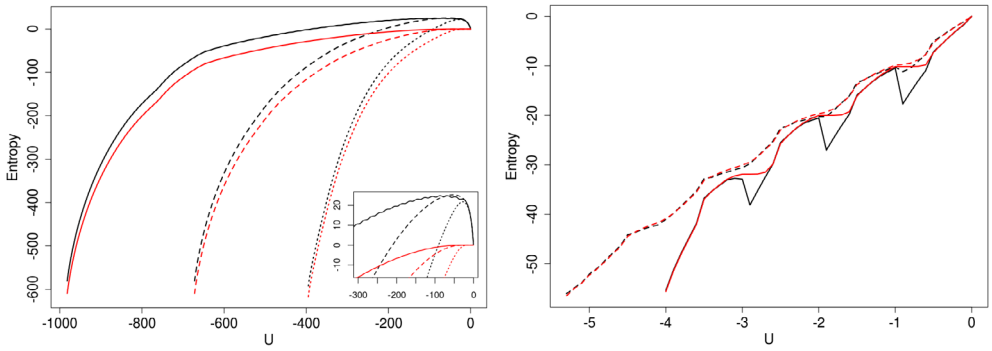

Fig. 1. The microcanonical entropy defined according to Boltzmann (black lines), $S_B(U)$, and to Gibbs (red lines), $S_G(U)$, vs. potential energy U for a SF-copolymer (left plot) and for poly-alanine (right plot). For both systems the entropy is shifted to have zero value at the maximal value of the potential energy (which is $U = 0$ for both models). For the SF-copolymer chain the block length is $b = 16$ and the values of the stiffness energy parameter are $\varepsilon_{st} = 0, 10, 20$, from the right to the left, i.e., dotted, dashed and solid lines, respectively. The inset shows the enlarged view at large energies, where oscillations both in S_B and in S_G are visible for the largest stiffness $\varepsilon_{st} = 20$. For the poly-alanine model data for chain lengths $N = 10$ and $N = 16$ are shown by the solid and the dashed lines, respectively.

We have

$$\Delta\mathcal{V} = \int_U^{U+\Delta U} dx = \int_U^{U+\Delta U} d\sigma dn$$
$$= \int_U^{U+\Delta U} d\sigma \frac{dn}{dU} dU \simeq \Delta U \int_U \frac{d\sigma}{|\nabla U|}, \tag{30}$$

where the last equality holds because $dU/dn = |dU/dn| = |\nabla U|$ for the orientation of the surface normal, $\hat{n}$, and considering that U only has a normal variation on the selected surface. The numerical realization for $g(U)$ in this case thus is closer to equation (5) than to equation (3) and for infinitesimal width of the energy interval it would actually approach the definition of the surface measure in equation (5). The same holds true when looking at $g(E)$ instead of $g(U)$, which is determined from the configurational density of states by an exact integration over the momentum variables. As discussed in the theory section, this calculation is still a local in energy definition of entropy, and we will continue in the following to use the term Boltzmann entropy and contrast it with the Gibbs entropy.

3 Results

3.1 Gibbs and Boltzmann entropies as a function of configurational energy

We start with an analysis employing the direct result of the Monte Carlo simulations, i.e., the density of states $g(U)$ for the configurational energy only. This is the way these simulations are commonly analyzed [15]. Comparing the Boltzmann and Gibbs entropy results for both models in Figure 1, an expected finding is that the Gibbs entropy is monotonously increasing with increasing energy, while the Boltzmann entropy goes through a maximum. Consequently, the inverse microcanonical temperature according to Boltzmann goes through zero at this maximum followed

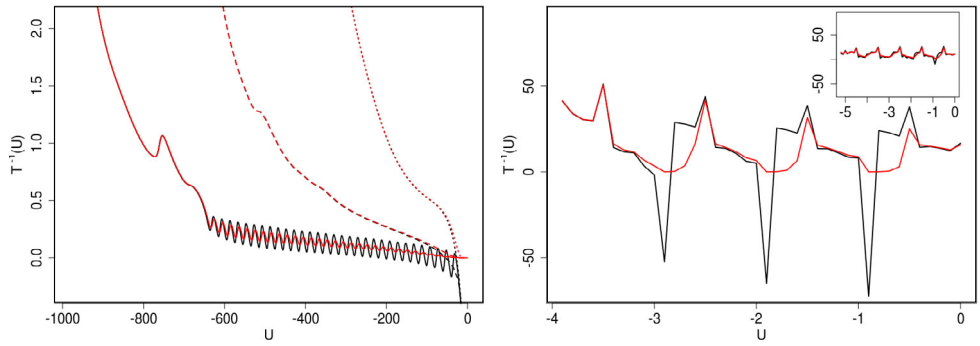

Fig. 2. The inverse microcanonical temperature defined according to Boltzmann (black lines) and to Gibbs (red lines) vs. potential energy U for SF-copolymer (left plot) and for poly-alanine (right plot) systems. The line style code is the same as in Figure 1, i.e., it encodes the intrachain stiffness for the SF-copolymer and the chain length for the poly-alanine model. The right plot shows the data for $N = 10$ while the inset shows the data for $N = 16$ separately, in order to avoid an overlap of curves in the graph. The scale of the y-axis is the same in the main plot and in the inset for better comparison of the amplitudes.

by a range of negative temperatures, while the inverse Gibbs temperature is strictly positive (see Fig. 2). Furthermore, both models share two important features in their energy spectra; the first is the fact that they are discrete, the second is the existence of two largely separate energy scales, at least if one chooses for the SF copolymer model a large stiffness parameter like is done for the leftmost lines in the left plot of Figure 1. This leads to undulations of the entropy in the high energy range, both for the Gibbs and the Boltzmann definition. This is more clearly seen for the poly-alanine model on the right of Figure 1. For the Boltzmann version the entropy has a series of maxima and minima, while the Gibbs entropy stays monotonic. With increasing the chain length, these features start to become smeared out. The mechanistic explanation for this behavior in the case of the SF copolymer was given in [35], for the poly-alanine it is the following: reducing the energy from zero means that hydrophobic contacts (strength $\varepsilon = 0.084$) have to be formed. Going from 11 such contacts to 12 and an energy close to -1 one could as well close 1 hydrogen bond with energy -1 and have 0 hydrophobic contacts, thereby largely increasing the configurational freedom of the chain and thus its number of states and entropy. The same happens when further hydrogen bonds are closed. This undulating behavior of the entropy has consequences for the behavior of the inverse microcanonical temperature shown in Figure 2. From the raw data in Figure 1 we can determine the Gibbs and Boltzmann microcanonical temperatures as discussed in the theory section. But note that we can not determine the derivative of the configurational entropy, $\ln g(U)$, with respect to the configurational energy, U, in an analytical fashion (or numerically as precisely as we wish), as we have a discrete spectrum for the configurational energy. So there is an arbitrariness in defining this numerical derivative by either the left step or the right step or the average one. This arbitrariness vanishes in the thermodynamic limit, as the density of points for the configurational energy per particle $u = U/N$ increases with $N \to \infty$ until we reach a continuous variation of u and arrive at a differentiable macroscopic configurational manifold and the thermodynamic relations defined between the differentials of the macroscopic variables. For small stiffnesses (the two right curves on the left plot in Figure 2) the predictions for the inverse microcanonical temperature using the Boltzmann and the Gibbs entropies are indistinguishable on the scale of the figure, except for energies close to zero, where T_B becomes negative. For both curves,

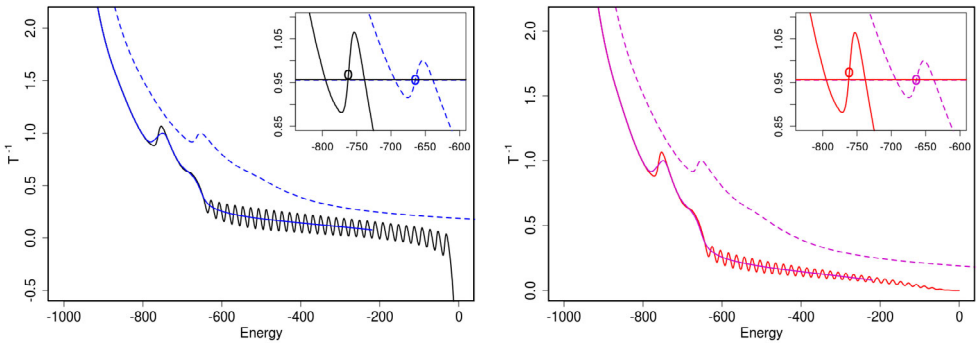

Fig. 3. Left plot: the inverse microcanonical temperature defined from the Boltzmann entropy in configuration space (solid black line, x-axis is U) and in phase space (dashed blue line, x-axis is E). The solid blue line depicts the data of the dashed blue line plotted as a function of the average configurational energy $\langle U \rangle$ at fixed total energy. Right plot: the inverse microcanonical temperature defined from the Gibbs entropy in configuration space (red solid line, x-axis is U) and in phase space (dashed magenta line, x-axis is E). The solid magenta line depicts the data of the dashed magenta line plotted as a function of the average configurational energy $\langle U \rangle$ at fixed total energy. The insets show the enlarged region of the 1st order transition with points indicating the temperatures at coexistence. All data are for the SF-copolymer chain with block length $b = 16$ and stiffness $\varepsilon_{st} = 20$.

the inverse temperature shows an inflection point at the continuous collapse transition of the model [34,36]. For the large stiffness, a first-order pseudo phase transition can be identified by the looped region in the curve, and again, the Gibbs and Boltzmann definitions agree in this regime. At larger energies the Boltzmann temperature shows an oscillatory regime created by individual bond angles which assume their energetically favorable angle range [35] (similar to closing hydrogen bonds in the poly-alanine model). The Gibbs temperature also shows these oscillations, but in a continuously more damped fashion as the energy increases, because it averages over larger and larger parts of configuration space with increasing energy. The poly-alanine inverse temperatures are zick-zack curves for both definitions, with the Boltzmann definition showing regions of negative temperature whenever a hydrogen bond closes. All the remarks by Hilbert, Dunkel and Hänggi [24,25] on the inability to predict energy flow from temperature for two bodies in contact for a non-invertible relation between temperature and energy are clearly applicable to this protein model system.

3.2 Gibbs and Boltzmann entropies as a function of total energy

When we consider the microcanonical ensemble we have to, however, work at constant total energy, not at constant configurational energy. The way to calculate the density of states in phase space, $g(E)$, from the density of states in configuration space, $g(U)$, is explained in the theory section. In Figure 3 we compare the result for the inverse microcanonical temperature in the SF copolymer model, $T^{-1}(E)$ to the result for $T^{-1}(U)$ shown in Figure 2, both for the Boltzmann definition (left plot) and the Gibbs definition (right plot). The same comparison is shown for the poly-alanine model in Figure 4. The first observation is that the range of oscillations in inverse temperature – a feature one would call an artefact for large thermodynamic systems – is absent now in both models and for both definitions of entropy. The convolution of energy contributions to the total energy from the discrete configurational

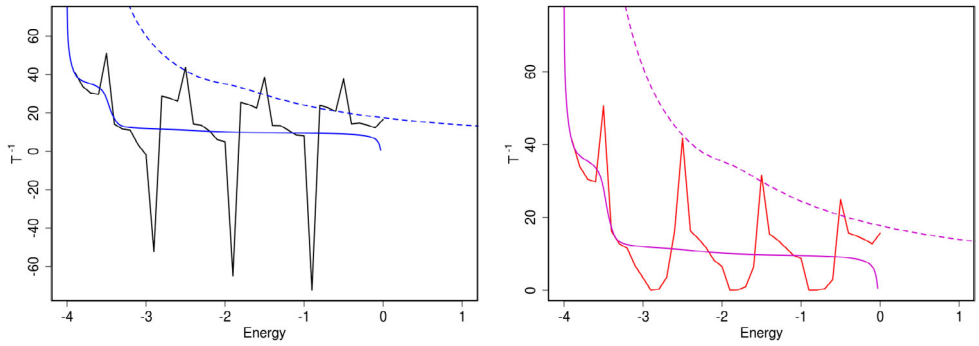

Fig. 4. The inverse microcanonical temperature defined from the Boltzmann entropy (left plot) and from the Gibbs entropy (right plot) both in configurational and in phase space. The color codes and the line style codes are the same as in Figure 3. All data are for the poly-alanine model chain of length $N = 10$.

Table 1. Inverse transition temperatures for the first order like transition in the SF copolymer model. Averages and error bars are obtained based on 10 independent determinations of $g(U)$.

definition	area U	infl. U	area E	infl. E
Boltzmann	0.957 ± 0.001	0.973 ± 0.003	0.955 ± 0.001	0.960 ± 0.001
Gibbs	0.957 ± 0.001	0.967 ± 0.004	0.955 ± 0.001	0.958 ± 0.001

energy and the continuous kinetic energy has smoothened the densities of states leading to well-behaved curves for $T^{-1}(E)$. More interestingly, the looped region for the first order transition in the SF copolymer model is shifted to the right (obviously, E is always larger than U) but occurs at the same height, i.e., at the same transition temperature. This is shown in more detail in the insets of Figure 3 where the horizontal lines indicate the Gibbs double tangent construction and the points are the inflection points in the transition region, which can also be used to determine the transition temperature [41]. All transition temperatures found in this way are listed in Table 1. Clearly, they agree very well with each other, except for the temperature determined from the second numerical derivative of the discrete configurational entropy where the numerical uncertainties add up.

Finally, Figures 3 and 4 contain a third data set. Here we plotted the inverse temperature $T^{-1}(E)$ against the average potential energy $\langle U \rangle(E)$ at fixed total energy. The range of potential energies U accessible at a given total energy E is $U_{\min} \leq U \leq \min(E, U_{\max})$, but different potential energies occur with different probabilities:

$$p(U|E) = \frac{(E-U)^{d/2-1} \cdot g(U)\Theta(E-U)}{\sum_{U'=U_{\min}}^{\min(E,U_{\max})} (E-U')^{d/2-1} \cdot g(U')}. \tag{31}$$

Using equation (31) one can calculate the mean configurational energy or its distribution for known configurational density of states function $g(U)$ and given total energy E. These two data sets, given by the full blue resp. magenta lines in the plots in Figure 3 and Figure 4 superimpose on the the predictions from the configurational entropy, but do not exhibit any of the unusual behavior – from the point of view of large system thermodynamics – found for the configurational entropy data. For the

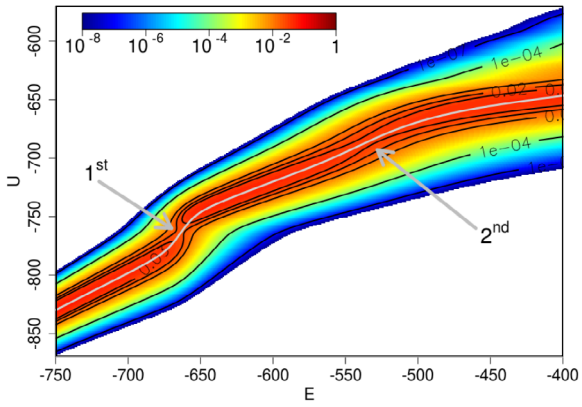

Fig. 5. Conditional probability $p\,(U|E)$ for the SF-copolymer chain with block length $b = 16$ and stiffness $\varepsilon_{st} = 20$. Both 1st and 2nd order transitions are visible.

poly-alanine system shown in Figure 4, this analysis allows to identify the continuous helix-coil transition in this model at low energies most clearly.

Figure 5 shows a color-coded height plot for the conditional probability of the configurational energy (Eq. (31)) at fixed total energy. The gray line represents the mean configurational energy, black lines are isolines. The conditional probability distribution $p\,(U|E)$ has an area with two maxima of probability in the range of the 1st order-like pseudo phase transition, whereas in the regime of the 2nd order-like transition just some widening of the distribution with a single maximum occurs. For large energies (not shown here) it reflects the oscillatory features of the configurational density function $g\,(U)$.

Finally we want to comment on the fact that the differences between the microcanonical temperatures obtained from Boltzmanns and Gibbs definition are well understood and are reflecting the behavior of the microcanonical specific heat [23,24] following from the Gibbs definition

$$\frac{T_G(E)}{T_B(E)} = 1 - \frac{1}{C_V^G(E)}\,, \tag{32}$$

which is defined as

$$C_V^G(E) = \frac{1}{1 - \frac{\Omega''\Omega}{\Omega'^2}}, \tag{33}$$

with Ω given by equation (7). In Figure 6 we confirm that our data comply with the exact result in equation (32).

3.3 Analysis and comparison of data for different conservation laws

The inverse microcanonical temperature according to Boltzmann and to Gibbs using different conservation laws is shown in Figure 7 for the SF-copolymer chain (block length $b = 16$ and stiffness $\varepsilon_{st} = 20$). Clearly, the overall influence of taking into account conservation of linear and angular momentum is very small for this system. However, taking into account the conservation of angular momentum leads to a visible shift of the looped region of the first order pseudo phase transition, as shown in the insets of Figure 7, while the influence of the conservation of linear momentum is hardly visible. The inverse transition temperature of the first order like transition

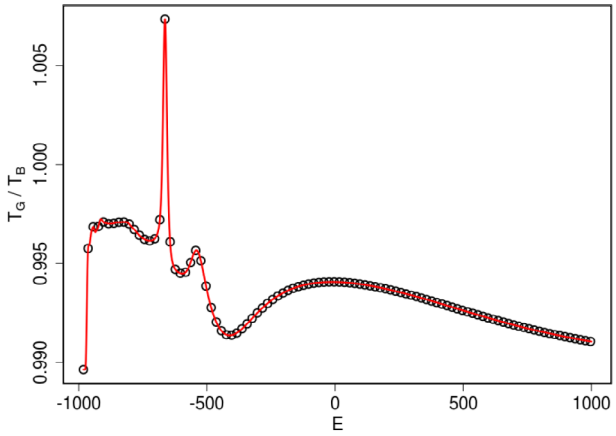

Fig. 6. Ratio of the inverse temperatures according to Boltzmann and to Gibbs for the SF-copolymer chain with block length $b = 16$ and stiffness $\varepsilon_{st} = 20$ shown by the red line. The function $1 - 1/C_V^G(E)$ is shown by black circles.

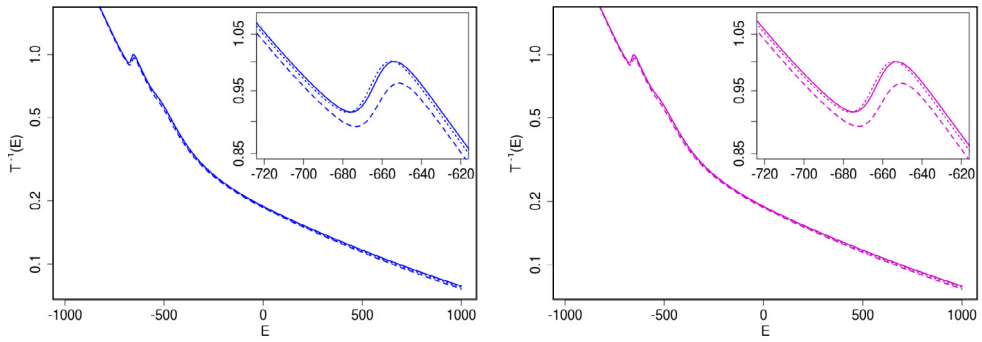

Fig. 7. The inverse microcanonical temperature according to Boltzmann (left plot) and to Gibbs (right plot) taking different conservation laws (full line: only energy conservation, dotted line: energy and linear momentum conservation, dashed line: energy, linear and angular momentum conservation) into account for the SF-copolymer chain (block length $b = 16$ and stiffness $\varepsilon_{st} = 20$). The insets show an enlarged view in the region of the 1st order transition.

in the presence of angular momentum conservation is $T^{-1}(E) = 0.925$, both for the Boltzmann and Gibbs entropy definitions, a noticable shift by $\Delta T_{tr} = 0.03$ compared to the results listed in Table 1. The calculation of the density of states in the presence of angular momentum conservation involves the determination of the inertia tensor of the particle distribution in space (see theory section), modifying the density of states in phase space. This quantity is shown in Figure 8 for the SF copolymer chain. It reflects the conformational changes of the chain giving rise to the oscillations in the inverse configurational temperature and has a kink in the range of configurational energies of the first order like pseudo phase transition, which seems to underly the shift observable in Figure 7. In Figure 9 the effects of the conservation laws on the pseudo phase transitions of the SF copolymer chain are analyzed using the microcanonical specific heat. For the region of the first order like transition the conclusions are the same as obtained from the inverse temperature. Conservation of linear momentum has little effect, while conservation of angular momentum leads to a visible shift of

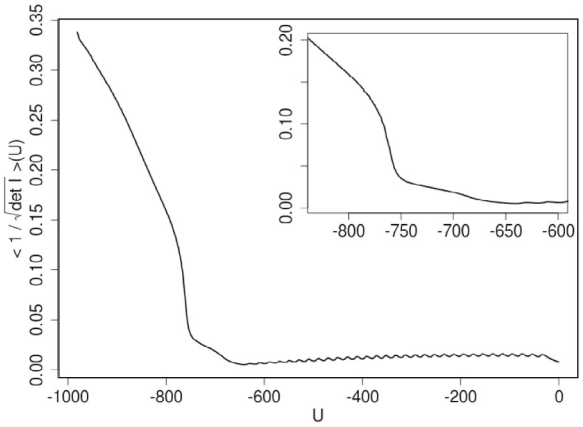

Fig. 8. The average of one over the square root of the determinant of the inertia tensor of the SF-copolymer as a function of configurational energy calculated using the Boltzmann entropy. The inset shows the enlarged region of the first order pseudo phase transition.

the transition temperature (as also shown in the insets on the left figures). The peak in the specific heat indicating the second order transition, however, shows shifts, both with linear momentum conservation (to the left) and with conservation of linear and angular momentum (to the right). Clearly, taking the conservation of angular momentum into account in addition to energy and linear momentum conservation has a non-negligible influence, at least for small systems. For large systems, all these effects will, of course, vanish.

4 Discussion and conclusions

We have presented an analysis of the microcanonical properties of two coarse-grained polymer models, a semi-flexible/flexible multiblock copolymer and an intermediate resolution model for poly-alanine, based on either the Boltzmann or the Gibbs definition of the microcanonical entropy. For finite systems, both definitions can lead to predictions, for instance for the microcanonical inverse temperature, which could be considered as artefacts when one has the behavior in the thermodynamic limit in mind. One such example is given by the fact, that the Boltzmann temperature gets negative for our models with a finite upper bound for the configurational energy, the other is given by the oscillatory regimes occurring in the $T^{-1}(E)$ curves for both models. However, these are well-defined and mechanistically understandable features of the models, and they vanish in the thermodynamic limit. The Gibbs entropy has the advantage that the associated microcanonical temperature stays positive for all energies by definition, and the entropy generally shows a smoother behavior as a function of energy, again by definition.

More importantly, when one takes into account that the microcanonical ensemble is not defined as a constant configurational energy ensemble but as a constant total energy ensemble, the "strange" microcanonical features discussed above all vanish. This is again due to an averaging procedure, as the number of states at fixed energy, E, is given by a convolution of the number of states at fixed configuration energy, U, with the number of states at the corresponding kinetic energy, $E - U$. Interestingly, and fortunately, conclusions on the location of pseudo phase transitions are little affected by the choice of entropy or total vs. configurational energy, at least for our model systems. As these possess 192 (SF copolymer) resp. 120 or 192

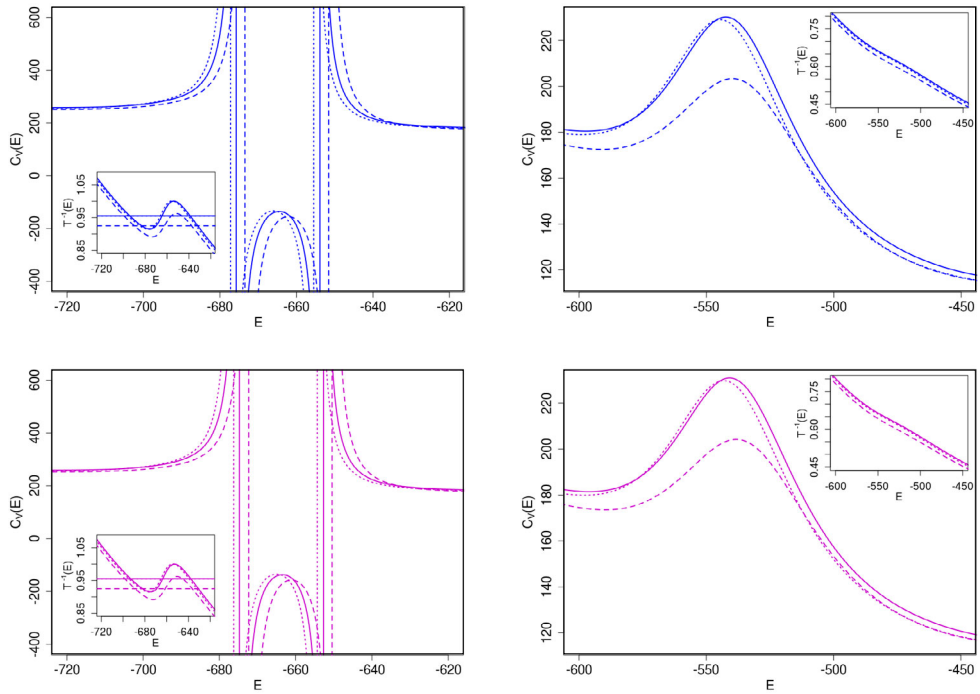

Fig. 9. The microcanonical specific heat according to Boltzmann (upper line) and to Gibbs (lower line) using different conservation laws (encoded by the same line styles as in Fig. 7). The regions of 1st order (left column) and 2nd order (right column) transitions are shown separately. The data are for the SF-copolymer chain (block length $b = 16$ and stiffness $\varepsilon_{st} = 20$). Insets show the inverse microcanonical temperatures in phase space according to Boltzmann and Gibbs).

(poly-alanine with $N = 10$ or $N = 16$) degrees of freedom in configuration space, we can conclude that the limiting behavior, where the choice of Gibbs vs. Boltzmann entropy does not matter any more, seems to be reached rather quickly. Of course, in a high precision determination of phase transition temperatures in the thermodynamic limit, a careful finite size scaling analysis would still show systematic trends [42].

We observed the strongest effect on an estimated transition temperature for a first order transition upon inclusion of angular momentum conservation as a constraint in the calculation of the densities of states (an observation also made in [43]). Linear momentum conservation had almost no effect. We argued that the strong effect of angular momentum conservation comes from a different weight which the density of states at fixed configurational energy obtains by the averaged square root of the inverse determinant of the inertia tensor, a quantity depending on the configuration of the system.

For continuous degrees of freedom, the property of the Gibbs entropy to be a mechanical adiabatic invariant for any system size N and not only in the thermodynamic limit, favors it over the Boltzmann entropy, if the latter is defined as the measure of a surface at constant energy (cf. Eq. (3) or Eq. (5)), which only possesses this property in the thermodynamic limit. The "Boltzmann" entropy calculated in numerical work for a continuous variation of energy values is actually by numerical necessity determined from an integral over the density of states (defined by Eq. (5)) over some small width ΔE. As a difference between two phase space volumes (contained within the

hypersurface of energy E and the hypersurface of energy $E + \Delta E$, respectively), which are both invariant under a given adiabatic process due to the adiabatic theorem, this is also an adiabatic invariant. Consequently, its logarithm is actually a type of local Gibbs entropy and also an adiabatic invariant for finite system sizes. Because of its locality in energy, it can lead to regimes of negative absolute temperature. However, at finite N, there are other, and perhaps more or equally important approximations usually taken, like the neglect of conservation laws every closed mechanical N-particle system necessarily possesses which lead to effects which are numerically as important as the different entropy definitions. And finally, there can occur problems with the arbitrariness of the transition from differentials to finite differences in the application of thermodynamic laws to finite sized systems.

The authors acknowledge funding by the German Science Foundation through SFB TRR102, sub-project A07, and project PA 473/10-1 as well as RFBR grant 13-03-91334-NNIO-a. The reported study was supported by the Supercomputing Center of Lomonosov Moscow State University [44] and the high-performance computer cluster at Martin Luther University. We were inspired to this study by a colloquium given by P. Hänggi in Halle in November 2015 and we acknowledge a long and constructive email discussion with him on questions of the adiabatic theorem and Gibss vs. Boltzmann entropies. And last but not least, we are indepted to W. Janke for a long-standing fruitful exchange of ideas.

References

1. B.A. Berg, Fields Inst. Comm. **26**, 1 (2000)
2. B.A. Berg, Comp. Phys. Comm. **147**, 52 (2002)
3. W. Janke, Physica A **254**, 164 (1998)
4. W. Janke, Lect. Notes Phys. **739**, 79 (2008)
5. F. Wang, D.P. Landau, Phys. Rev. Lett. **86**, 2050 (2001)
6. F. Wang, D.P. Landau, Phys. Rev. E **64**, 056101 (2001)
7. T. Wuest, Y.W. Li, D.P. Landau, J. Stat. Phys. **144**, 638 (2011)
8. F. Liang, J. Stat. Phys. **122**, 511 (2006)
9. F. Liang, C. Liu, R.J. Carroll, J. Amer. Stat. Ass. **102**, 305 (2007)
10. F. Liang, Statist. Prob. Lett. **79**, 581 (2009)
11. D.H.E. Gross, *Microcanonical Thermodynamics: Phase Transitions in "Small" Systems* (World Scientific, Singapore, 2001)
12. C. Junghans, M. Bachmann, W. Janke, Phys. Rev. Lett. **97**, 218103 (2006)
13. W. Janke, Nucl. Phys. B (Proc. Suppl.) **63A-C**, 631 (1998)
14. W. Paul, F. Rampf, T. Strauch, K. Binder, Comp. Phys. Commun. **178**, 17 (2008)
15. W. Janke, W. Paul, Soft Matter **12**, 642 (2016)
16. R.S. Ellis, *Entropy, Large Deviations and Statistical Mechanics* (Springer, Berlin, 2006)
17. H. Touchette, Phys. Rep. **478**, 1 (2009)
18. P. Hertz, Ann. Phys. **33**, 225 (1910)
19. P. Hertz, Ann. Phys. **33**, 537 (1910)
20. J.W. Gibbs, *Elementary principles of statistical mechanics* (Charles Scribner's Sons, New York, 1902)
21. J. Dunkel, S. Hilbert, Physica A **370**, 390 (2006)
22. S. Hilbert, J. Dunkel, Phys. Rev. E **74**, 011120 (2006)
23. J. Dunkel, S. Hilbert, Nature Phys. **10**, 67 (2014)
24. S. Hilbert, P. Hänggi, J. Dunkel, Phys. Rev. E **90**, 062116 (2014)
25. P. Hänggi, S. Hilbert, J. Dunkel, Phil. Trans. Roy. Soc. A **374**, 20150039 (2016)
26. R.H. Swendsen, J.S. Wang, Phys. Rev. E **92**, 020103 (2015)
27. D. Frenkel, P. Warren, Am. J. Phys. **83**, 163 (2015)
28. P. Ehrenfest, Phil. Mag. **23**, 500 (1917)
29. T. Levi-Civita, Abhandl. Mathem. Semin. Hamburg **6**, 323 (1928)

30. A.I. Khinchin, *Mathematical Foundations of Statistical Mechanics* (Dover Publications, New York, 1949)
31. V.L. Berdichevskii, J. Appl. Math. Mech. **52**, 738 (1988)
32. P. Schierz, J. Zierenberg, W. Janke, J. Chem. Phys. **143**, 134114 (2015)
33. P. Schierz, J. Zierenberg, W. Janke, Phys. Rev E **94**, 021301(R) (2016)
34. S.V. Zablotskiy, J.A. Martemyanova, V.A. Ivanov, W. Paul, J. Chem. Phys. **144**, 244903 (2016)
35. S.V. Zablotskiy, V.A. Ivanov, W. Paul, Phys. Rev. E **93**, 063303 (2016)
36. S.V. Zablotskiy, J.A. Martemyanova, V.A. Ivanov, W. Paul, Polym. Sci. Ser. A **58**, 899 (2016)
37. M. Cheon, I. Chang, C.K. Hall, Proteins: Struct. Funct. Bioinf. **78**, 2950 (2010)
38. A. Voegler Smith, C.K. Hall, Proteins: Struct. Funct. Bioinf. **44**, 344 (2001)
39. B. Werlich, M.P. Taylor, W. Paul, Phys. Proc. **57**, 82 (2014)
40. B. Werlich, T. Shakirov, M.P. Taylor, W. Paul, Comp. Phys. Commun. **186**, 65 (2015)
41. S. Schnabel, D.T. Seaton, D.P. Landau, M. Bachmann, Phys. Rev. E **84**, 011127 (2011)
42. J. Zierenberg, W. Janke, Phys. Rev. E **92**, 012134 (2015)
43. M.P. Taylor, K. Isik, J. Luettmer-Strathmann, Phys. Rev. E **78**, 051805 (2008)
44. V. Sadovnichy, A. Tikhonravov, V. Voevodin, V. Opanasenko, in *"Contemporary High Performance Computing: From Petascale toward Exascale"* (Chapman & Hall/CRC Computational Science, Boca Raton, USA, CRC Press, 2013), pp. 283–307